

Early-Life Adversity–Induced Epigenetic Reprogramming of Prefrontal Cortex in Rats Subjected to Maternal Separation

Aleena Francis, Lauren Allen McKibben, and Yogesh Dwivedi

ABSTRACT

BACKGROUND: Early-life adversity (ELA) can lead to long-lasting behavioral and neurobiological changes through epigenetic mechanisms. In this study, we comprehensively mapped genome-wide DNA methylation in the prefrontal cortex of rats following maternal separation (MS).

METHODS: Rat pups were separated from their mother for 180 minutes/day from postnatal days (PNDs) 1 to 14 and tested for depressive- and anxiety-like behavior during adulthood (PNDs 80–89). Genome-wide DNA methylation, corresponding functional analyses, and transcription factor binding sites (TFBSs) were performed using reduced-representation bisulfite sequencing, focusing on differentially methylated cytosines (DMCs), differentially methylated regions (DMRs), and non-CpG sites.

RESULTS: Both male and female MS rats showed a significant decrease in sucrose preference. Principal component and multidimensional scaling analyses did not show differences in the methylation data between male and female rats, prompting us to combine them in subsequent analyses. A total of 33,905 DMCs and 151 DMRs were identified in the MS group. The functional analysis of the dysregulated genes by DMCs and DMRs in the promoter or gene body revealed gene enrichment involved in neurodevelopment, synaptic plasticity, and stress response. Key genes with altered methylation included *Dnmt3a/b*, *Notch1*, *Mapk14*, and calcium channel subunits. Gene network analysis revealed interactions among ribosomal, MAPK (mitogen-activated protein kinase), and glutamatergic pathway genes. An enrichment of Elk1 TFBSs was particularly noted within the DMR. Additionally, differential non-CpG methylation, specifically at CHH (H = C/T/A) sites, dysregulated the Wnt pathway genes.

CONCLUSIONS: Our findings expand our understanding of the molecular mechanisms that underlie the long-term effects of ELA and identify potential biomarkers for stress-related psychiatric disorders.

<https://doi.org/10.1016/j.bpsgos.2025.100487>

During early life, intense and stressful events can significantly impact an individual's brain development, synaptogenesis, synapse pruning, and cognitive maturation. These effects can have a lasting impact on behavioral capabilities later in life (1,2). Early-life adversity (ELA) refers to exposure to stressful environmental circumstances such as parental separation, physical violence, emotional neglect, and starvation during the developmental period (3). Nearly one half of children worldwide experience some kind of ELA (4,5) and therefore are at a significantly higher risk of developing adverse outcomes in adulthood, including major depressive disorder, posttraumatic stress disorder, social phobia, generalized anxiety disorder, panic disorder, and substance use disorders (6).

The impact of ELA on mental health has been a subject of considerable research interest (7–11). Maternal separation (MS) is a well-known rodent model for investigating the effects of ELA, which parallels child abuse and/or neglect in humans. Studies have shown that MS can emulate the neurobiological effects of ELA in humans, leading to the development of mood and anxiety disorders in adulthood (12). MS can trigger

neuroinflammatory responses in the brain, which can disrupt the normal development and functioning of the brain (13), causing irreversible damage to offspring by stimulating neuronal apoptosis and altering neuroplasticity (14). Additionally, MS affects the neuroendocrine system, including the hypothalamic-pituitary-adrenal axis, the sympathetic-adrenal-medullary system, and the central dopamine system. Dysregulation of these systems can lead to abnormal levels of stress hormones and neurotransmitters, impacting the body's stress response (15).

The field of epigenetics has emerged as a crucial area of study for understanding the relationship between ELA and psychiatric illnesses (1,16–19). Among the various epigenetic mechanisms, DNA methylation has received considerable attention in psychiatric research by mediating long-term programming effects. DNA methylation typically occurs at CpG sites within gene promoters and is associated with transcriptional silencing in mammalian genomes, while gene body methylation is positively correlated with the expression (20). On the other hand, the implications of 5mC (5-methylcytosine) methylation in other genomic regions remain poorly understood.

Previous studies have shown that MS alters DNA methylation patterns in brain areas that are crucial for learning and memory. For example, a study demonstrated that neonatal MS exposure elicited enduring DNA methylation changes, specifically within the rat hippocampus, indicating a potential mechanism by which early adversity can disrupt cognitive development (21). Another investigation revealed that MS induced differential methylation at the *BDNF* exon I promoter within the hippocampus and medial prefrontal cortex (PFC) and linked these changes to the enduring neurobiological consequences of stress (22). Given the established associations between MS, DNA methylation, and behavioral outcomes, recent advances in sequencing techniques provide invaluable tools for elucidating the specific methylation alterations associated with MS. The current study was undertaken to examine genome-wide DNA methylation in the PFC of MS rats with the central hypothesis that MS-induced behavioral changes would be correlated with alterations in DNA methylation in both promoter regions and gene bodies, leading to changes in gene functions and associated pathways. Our findings deepen the understanding of the molecular mechanisms that underlie the long-term effects of ELA and highlight potential epigenetic biomarkers and therapeutic targets.

METHODS AND MATERIALS

Animals

Detailed experimental protocols are provided in the Supplement. This study utilized Sprague Dawley rats (*Rattus norvegicus*), and experiments were approved by the Institutional Animal Care and Use Committee at the University of Alabama at Birmingham. As previously reported by our group (23), MS pups were separated from dams into individual cages on a 30 °C heating pad for 180 minutes each day on postnatal days (PNDs) 1 to 14. On the same days as MS, control pups were handled for 5 minutes twice daily and returned to the dam. Following PND 14, all dams and litters were transferred to fresh cages until weaning on PND 21.

Behavioral Tests

Behavioral tests were conducted in a blind fashion. In adulthood (PND 80), a sucrose preference test, elevated plus maze, and forced swim test were conducted following our previous study (24) in order to measure anhedonia (25), anxiety-related behavior (26), and depressive-like behavior (27), respectively. All behaviors were compared across groups using 2×2 analysis of variance (ANOVA). Data are reported as mean \pm SEM. To examine epigenetic changes related to anhedonia, we selected 10 MS rats (5 per sex) with the lowest percentage sucrose preference level and randomly chose 10 control rats for the methylation study. In each group, rats selected for reduced-representative bisulfate sequencing (RRBS) were from multiple litters.

Brain Collection

Twenty-four hours following the behavioral experiments, animals were sedated under isoflurane inhalation and euthanized by decapitation. Prefrontal cortices were dissected and

immediately placed on liquid nitrogen. Samples were stored at -80°C until DNA isolation.

DNA Isolation/Quality Control. Genomic DNA was extracted from the PFC using the QIAamp genomic DNA extraction kit (Qiagen). The concentration of extracted genomic DNA was measured with NanoDrop (Thermo Fisher Scientific), and the OD260/OD280 ratio was used for detecting any residual contaminants in DNA preparation.

Reduced-Representative Bisulfate Sequencing

The DNA library was prepared using the NuGEN Ovation RRBS Methyl-seq kit (Tecan Genomics), with 20 ng/ μL of DNA. Subsequent to *MspI*-based digestion, bisulfite conversion, and polymerase chain reaction amplification, sequencing was performed with NovaSeq500 in the 75-bp single-end reads mode (Illumina).

RRBS Data Analysis

Filtering of RRBS reads and detailed analysis are provided in the Supplement. The filtered reads were mapped against the *R. norvegicus* reference genome using bsmmap, and the methylation calling at CG, CHG, and CHH sites ($H = A/C/T$ bases) was performed with mcall using default parameters. The differential methylation in the MS group relative to the control group was analyzed, and the significant sites and regions were selected with mcomp, which uses Fisher's exact test for significance assessment.

Functional Analysis

The functional enrichment analysis was carried out using the enrichR package with p value $\leq .05$. The known interaction network was assessed using the STRING database and visualized using Cytoscape version 3.10.2. The gene expression profiles in different tissues were accessed via the RatGTEx portal (<https://ratgtex.org/>). The expression profile used for correlation analysis with the methylation data was obtained from Benekareddy *et al.* (28), as detailed in the Supplement.

Transcription Factor Binding Site Enrichment

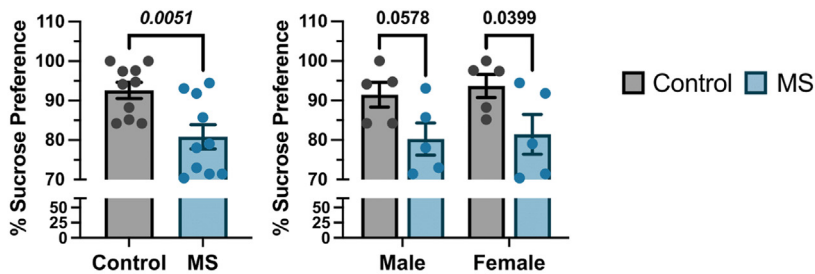
Transcription factor binding sites (TFBSs) in the differentially methylated regions (DMRs) were determined and tested for enrichment of known/de novo vertebrate TF binding motifs using the findMotifsGenome.pl script from the HOMER package (29) with the following parameters: -masked -size 200 -len = 8,10,12.

RESULTS

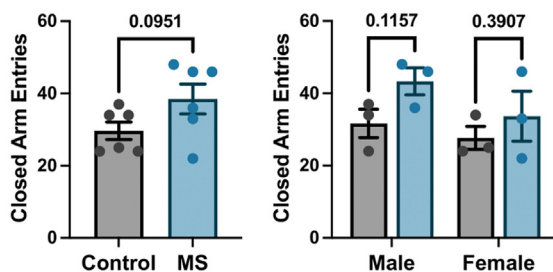
Animal Behavior

The sucrose preference percentage was significantly lower in MS-exposed adult male and female rats than in control rats (control mean \pm SD = 92.57 ± 6.490 , MS = 80.84 ± 9.653 ; $t_{18} = 3.190$, $p = .0051$, $R^2 = 0.36$) (Figure 1A). The interaction between sex and MS was not significant (2-way ANOVA: $F_{1,16} = 0.0186$, $p > .05$) (Figure 1A). The average number of closed-arm entries in the elevated plus maze was slightly higher in the MS group (38.50 ± 10.11) than in the control group (29.67 ± 5.955), but this effect was not significant ($t_{10} =$

A Sucrose Preference Test



B Elevated Plus Maze



C Forced Swim Test

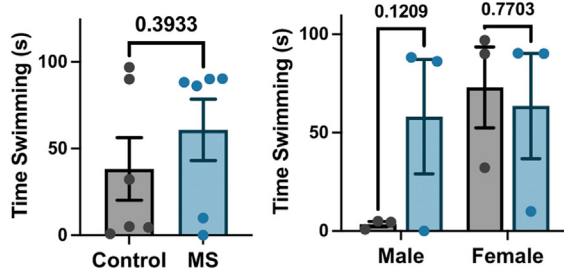


Figure 1. Animal behavioral changes associated with MS. **(A)** Sucrose preference test. MS significantly reduced sucrose preference, indicating anhedonia-like behavior. **(B)** Elevated plus maze. The number of entries into the closed arms was recorded as an indicator of anxiety-related behavior. **(C)** The time (in seconds) spent swimming during the forced swim test was used to assess depressive-like behavior. Data are reported as mean \pm SEM. MS, maternal separation.

1.843, $p = .0951$) (Figure 1B). The effect of MS on closed-arm entries did not depend on sex (2-way ANOVA: $F_{1,8} = 0.3672$, $p > .05$) (Figure 1B). Finally, neither MS alone ($t_{10} = 0.8921$, $p > .05$) nor its interaction with sex (2-way ANOVA: $F_{1,8} = 2.075$, $p > .05$) significantly affected forced swim behavior (Figure 1C).

RRBS Findings

RRBS was done to examine the methylation differences between MS and control rats. Ten samples, each from 5 male and 5 female rats, were sequenced for the control and MS groups. Except for 1 sample (MS6/MSM1), all exhibited an alignment rate $>90\%$ against the rat reference genome. Therefore, MS6/MSM1 was excluded from further analysis (Table S1). The total number of CpG sites identified with a minimum depth of 20 was >3 million in both groups. Initially, we conducted principal component analysis and multidimensional scaling of the methylated CpG sites to evaluate sample variability (Figure S1A, B). The findings revealed distinct clustering of the control and MS groups, indicating variability within each group regardless of sex. Notably, no sex-specific variation was observed in the control group. Therefore, the sex cohorts were merged for the differential analysis. Also, the distribution of all

methylated sites in both the control and MS samples revealed that 30.2% and 30.7% of methylated cytosines were located within CpG islands, while 22.9% and 23.1% were situated on the shore, and 11% and 11.1% were found in shelf regions, respectively, suggesting that there was an ample number of methylated CpG sites with functional implications for studying differential methylation in MS (Figure S1C, D). The schematic workflow of the subsequent differential methylation analysis is provided in Figure S2.

Differentially Methylated CpG Sites

We initially focused on CpG sites and found 33,905 significant differentially methylated CpGs when the MS group was compared with the control group. (Figure 2A and Table S2). Among the differentially methylated cytosines (DMCs), 7358 had strong hypomethylation, and 8851 had strong hypermethylation. Nevertheless, the majority of DMCs were classified as hypermethylated (Figure 2B). A volcano plot depicts the significant strong hyper/hypomethylated cytosines at CpG dinucleotides (Figure 2C). The top 50 strongest hyper/hypo-DMCs are shown in Table S3, and a heatmap illustrates the methylation levels of these DMCs in each of the control and MS samples (Figure 2D).

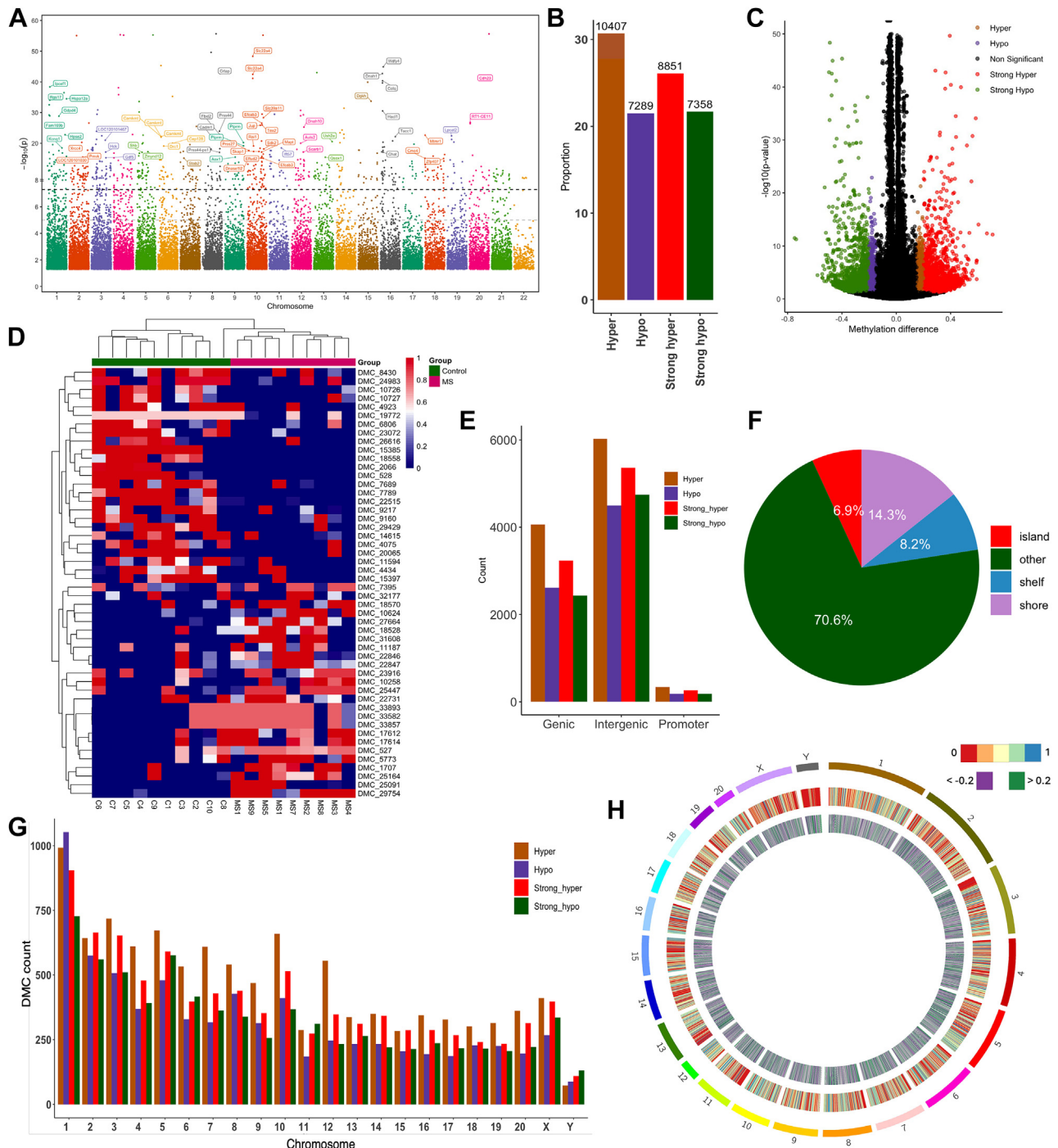


Figure 2. Differentially methylated sites. **(A)** Genomic coordinate dot plot (Manhattan plot) of the MS-associated CpG methylation detected. The x-axis represents chromosomes ranked by number, the y-axis represents $-\log_{10}(p \text{ values})$, and the dotted line indicates the significance level. **(B)** Bar chart represents the distribution of hyper- and hypomethylated sites among all 33,905 significant DMCs. **(C)** A volcano plot of all the methylated sites with significant ($p < .05$) strong hyper-DMCs (>0.3 ; highlighted as red) and strong hypo-DMCs (-0.3 ; highlighted as green). Hyper- and hypomethylated sites are colored brown and purple, respectively. **(D)** Heatmap depicting the methylation level of the top 50 differentially methylated sites between the MS and control groups. The samples and DMC sites were clustered using the hierarchical clustering algorithm. The control group samples are clustered under green, and MS samples are clustered under violet. **(E)** DMC distribution among genic, intergenic, and promoter regions. **(F)** Distribution of DMCs in the CpG island, shore, and shelf regions. Islands are denoted by red, shores (regions 0–2 kb upstream and downstream from CpG Islands) are denoted by blue; the other (genomic region that falls outside of the CpG islands, shores, and shelves) is denoted by green. **(G)** DMC chromosomal distribution. The bar plot representing strong hyper- (>2 , red), strong hypo- (<-2 , green), hyper- (≤ 0.2 and >0.15 ,

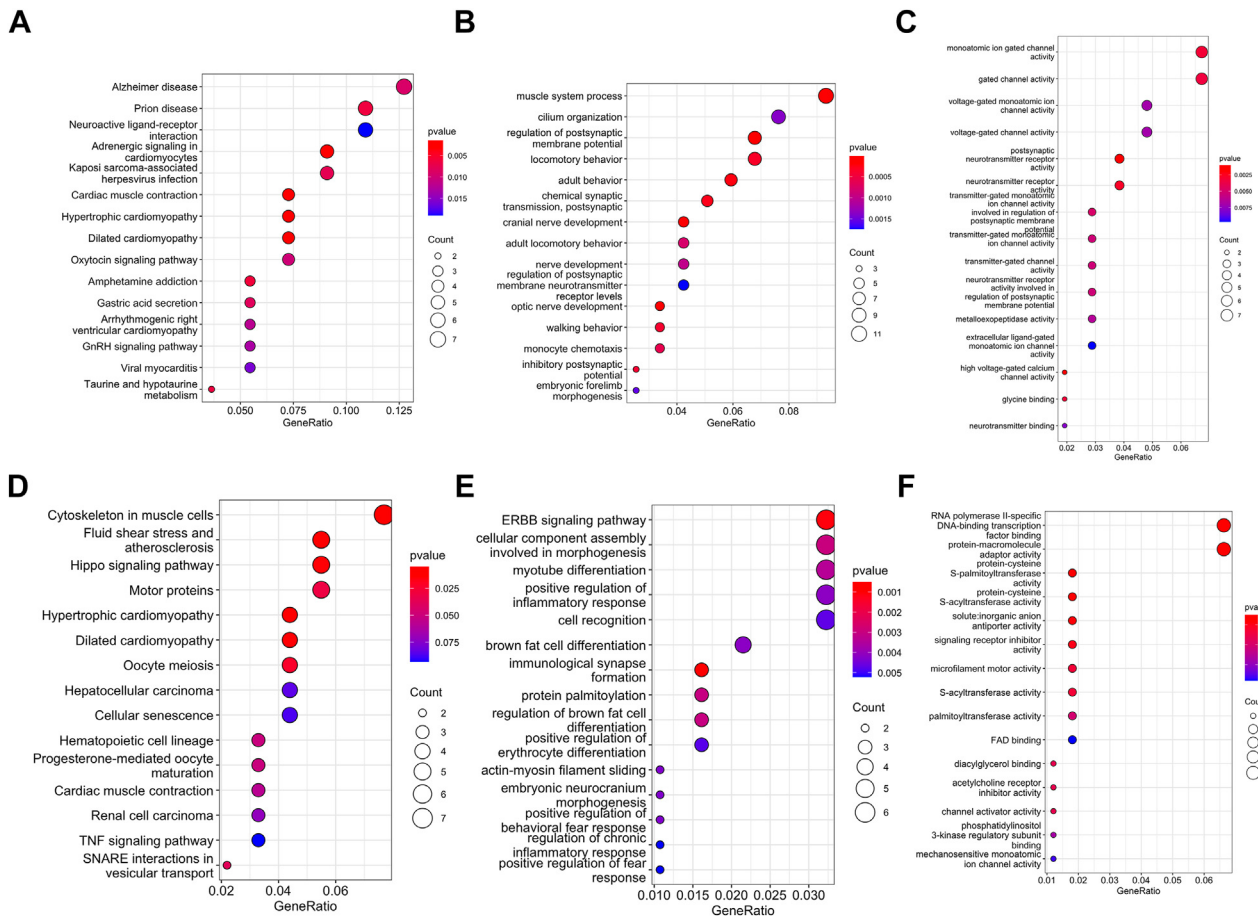


Figure 3. Functional enrichment analysis of genes regulated by strong hypomethylated promoters. **(A)** The KEGG pathways enriched among the genes regulated by strong hypomethylated promoters. **(B)** The enriched biological process terms among the genes regulated by strong hypomethylated promoters. **(C)** The enriched molecular function terms among the genes regulated by strong hypomethylated promoters. **(D)** The KEGG pathways enriched among the genes regulated by strong hypermethylated promoters. **(E)** The enriched biological process terms among the genes regulated by strong hypermethylated promoters. **(F)** The enriched molecular function terms among the genes regulated by strong hypermethylated promoters. GnRH, gonadotropin-releasing hormone; KEGG, Kyoto Encyclopedia of Genes and Genomes; TNF, tumor necrosis factor.

The distribution of identified DMCs within annotated genome regions indicates that the intergenic region contained the highest number of DMCs. However, within the genomic regions with functional implications, such as coding and regulatory areas, the majority of DMCs were found within genic regions (12,341) (Table S4). The fewest DMCs were identified in the promoter region (963) (Figure 2E and Table S5). A significant enrichment relative to expected values was observed for the DMCs in both the genic and promoter regions using a $p < .01$; however, the intergenic region had fewer DMCs than expected.

The regions of DNA with a high density of CpG dinucleotides, known as CpG islands, together with the extended shores and shelves often found in proximity to gene promoters, play a vital role in gene regulation through

methylation. Among the significant DMCs identified in the MS group, most overlapped with CpG shore (4854), followed by shelf (2795) and island (2334) (Figure 2F).

The hyper- and hypomethylated sites were distributed across the chromosomes, highlighting their diverse genomic locations (Figure 2G and Supplemental Results). Furthermore, no direct correlation was observed between gene density and the DMC sites, except on chromosome Y, where the DMCs were spread across regions of low gene density (Figure 2H). Interestingly, 2 of the mammalian de novo DNA methyltransferases, *Dnmt3a* and *Dnmt3b*, were found to be differentially methylated in the MS group. A strong hypomethylation of the CpG site at the third intron was observed in *Dnmt3a*, and a strong hypermethylation in the coding DNA sequence region was identified in *Dnmt3b* (Supplemental Results).

← brown), and hypo- (≥ -0.2 and < -0.15) methylated site frequency across the rat genome. **(H)** Circos plot depicting the DMC distribution across chromosomes. The first track shows gene density within a 500-kb window, and the second track depicts differentially methylated sites that have been plotted. C, control; DMC, differentially methylated cytosine; MS, maternal separation.

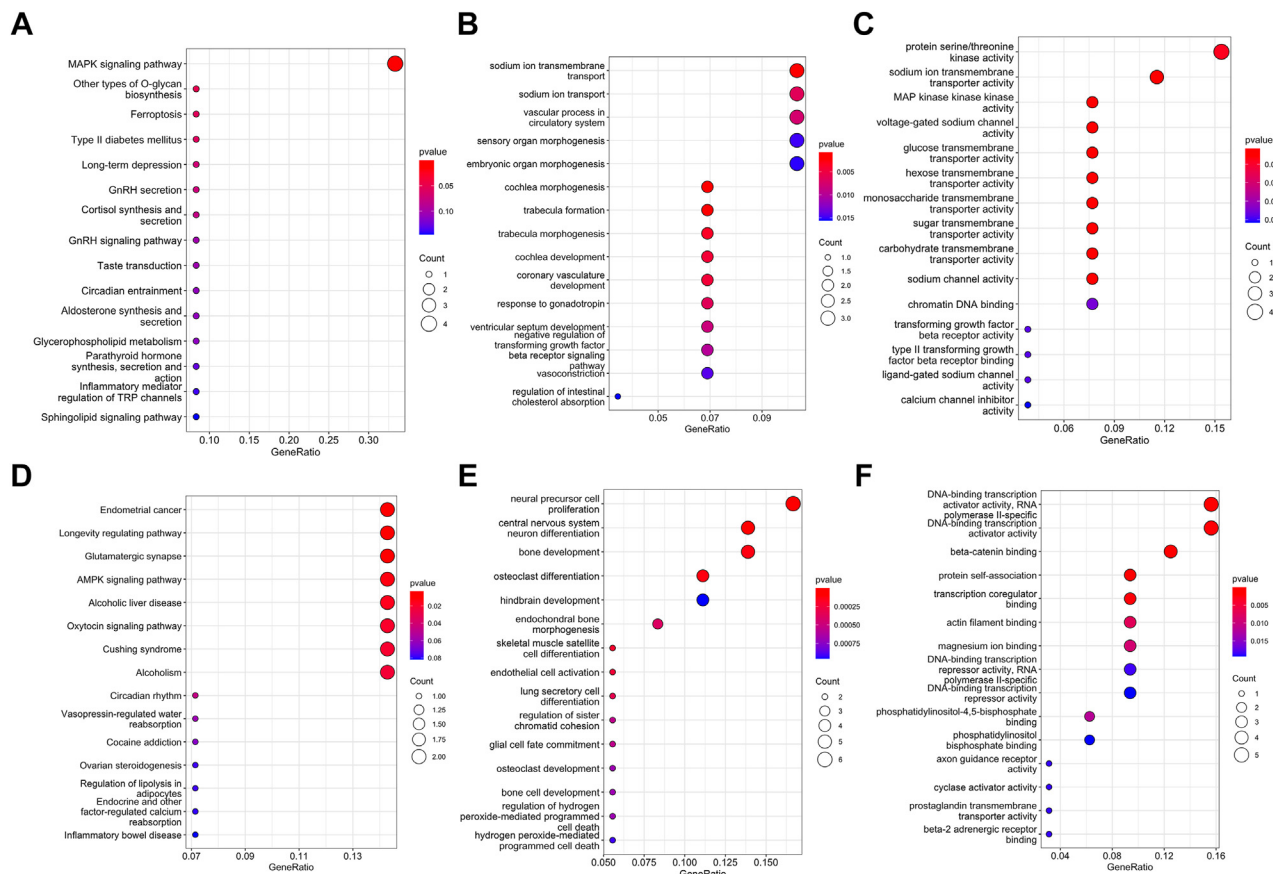


Figure 4. Functional enrichment analysis of the genes with gene body differential methylation. **(A)** The KEGG pathways enriched among the genes having strong hypomethylation. **(B)** The KEGG pathways enriched among the genes having strong hypermethylated cytosines. **(C)** The enriched biological process terms among the genes having strong hypomethylated cytosines. **(D)** The enriched biological process terms among the genes having strong hypermethylated cytosines. **(E)** The enriched molecular function terms among the genes having strong hypomethylated cytosines. **(F)** The enriched molecular function terms among the genes having strong hypermethylated cytosines. ABC, ATP-binding cassette; cAMP, cyclic adenosine monophosphate; cGMP, cyclic guanosine monophosphate; ECM, extracellular matrix; GnRH, gonadotropin-releasing hormone; GTPase, guanosine triphosphatase; KEGG, Kyoto Encyclopedia of Genes and Genomes; MAPK, mitogen-activated protein kinase; mTOR, mechanistic target of rapamycin.

Functional Characterization of DMCs

Functional Enrichment of Genes Regulated by the Differentially Methylated Promoters. Because hypermethylated promoters induce heterochromatin formation and hinder the binding of transcription activators, consequently repressing gene expression, it is imperative to investigate the functional implications of both hyper- and hypomethylated promoters. Functional analysis revealed that the hypomethylated promoters were enriched with neuroactive ligand-receptor interaction and oxytocin signaling pathways (Figure 3A). Among biological processes, the regulation of postsynaptic membrane potential, chemical synaptic transmission, and postsynaptic and nerve development were enriched (Figure 3B). Molecular functions included postsynaptic neurotransmitter receptor activity, monoatomic ion-gated channel activity, and high voltage-gated calcium channel activity (Figure 3C and Table S6).

The functional analysis of the hypermethylated promoter genes in MS group rats showed an enrichment of the Hippo signaling, motor proteins, and SNARE interactions in vesicular transport pathways (Figure 3D). The biological processes

included immunological synapse formation, positive regulation of inflammatory response, and behavioral fear response (Figure 3E). Molecular functions such as signaling receptor inhibitor activity and acetylcholine receptor inhibitor activity were found to be enriched in the hypermethylated promoter genes (Figure 3F and Table S7).

Functional Enrichment of the Genes Containing DMCs. Functional analysis was also performed on genes containing differentially methylated sites within the gene body. Methylation within gene loci was positively correlated with higher gene transcription levels. Moreover, gene body methylation may influence various cellular processes, including histone modification, alternative splicing, and the occurrence of spurious transcription (20). We identified 46 genes associated with the MAPK signaling pathway that exhibited strong hypomethylation, while another 40 genes displayed strong hypermethylation in gene body CpG sites. In the glutamatergic synapse pathway, 25 genes exhibited strong hypomethylation, while 20 genes displayed significant hyper-DMCs within their gene body (Figure 4A, B).

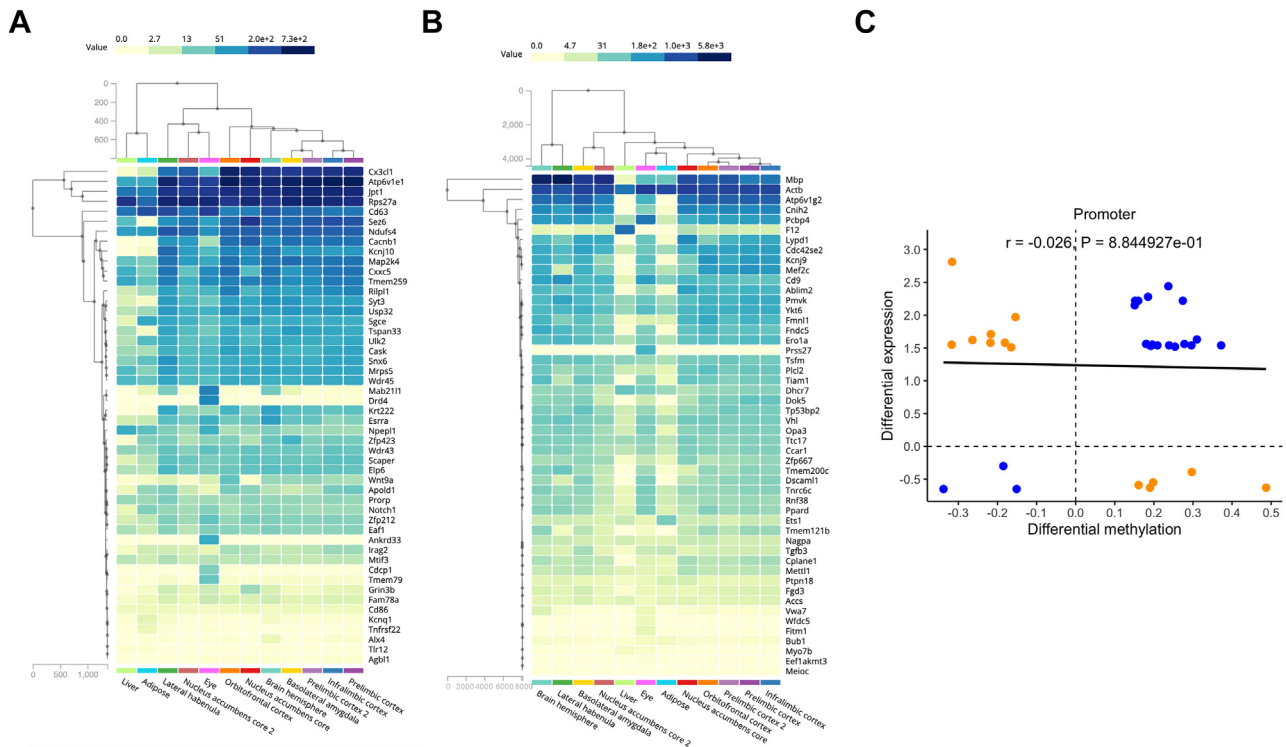


Figure 5. The gene expression profile of the top 50 DMCs containing promoters obtained from the RatGTEx database. **(A)** Strong hypomethylated. **(B)** Strong hypermethylated. **(C)** Correlation of methylation levels with the expression profile of genes harboring promoter DMCs. Scatter plot and Pearson's correlation showing the correlation between the differences in mRNA expression and methylation. The line represents a linear regression. Blue and orange dots represent the mRNA-DMC pairs exhibiting positive or inverse relationships, respectively. DMC, differentially methylated cytosine; mRNA, messenger RNA.

The genes containing hypo-DMCs were notably enriched in pathways associated with aldosterone synthesis and secretion and long-term depression, while genes with hyper-DMCs exhibited significant enrichment in pathways related to calcium signaling, GABAergic (gamma-aminobutyric acid) synapses, and mTOR (mechanistic target of rapamycin) signaling (Figure 4A, B). The dendrite development, postsynapse organization, and small GTPase-mediated signal transduction genes were enriched among hypo-DMCs (Figure 4C). Conversely, actin filament organization, regulation of presynaptic membrane potential, visual system development, and sensory system development genes were found to be hypermethylated within the gene body under MS conditions (Figure 4D). Among the molecular function terms, the ion channel and calcium channel regulator activity genes had hypo-DMCs. In contrast, transmembrane receptor protein tyrosine kinase activity, ubiquitin protein ligase binding, and ABC-type transporter activity genes were found to be harboring hyper-DMCs (Figure 4E, F; Tables S8 and S9).

Tissue-Level Expression Analysis of Genes

Because the gene expression patterns across normal tissues delineate the typical sites of expression, dysregulation of these patterns can significantly impact the specific tissues in which the genes are expressed. Therefore, we first examined the expression profiles of genes regulated by differentially methylated promoters (Figure 5A, B and Table S10). The correlation analysis of our methylation data with the differential gene

expression profiles from Benekareddy *et al.* (29) indicated a negative correlation of -0.026 ($p = .8$). This lack of statistical significance is likely attributable to the limited overlap of only 33 genes (Figure 5C). Among these, *Dscaml1*, *Tiam1*, and *Sema7a* exhibited promoter hypermethylation and showed reduced gene expression in MS. Conversely, hypomethylation in the promoters of *Rps27a*, *Apobec1*, *Cd63*, *Clasp1*, and *Alx4* was associated with a positive trend in gene expression.

We further investigated the expression levels of genes containing DMCs within the gene body to discern tissue-specific expression patterns (Figure 6A, B and Table S11). A moderately significant positive correlation was observed between the differential methylation of gene body and gene expression patterns from the previous study (0.106 , $p = .055$) (Figure 6C). The genes *Flt1*, *Rapgef1*, *Tiam1*, *Zc3h8*, *Dscaml1*, *Mybn*, and *Tgfb3* exhibited strong hypomethylation and were associated with expression downregulation. In contrast, the genes *Cd47*, *Necap2*, *Stk38*, *Gab1*, *Ldlrad3*, *Prom1*, *Ppp3ca*, *Pcbp4*, *Snf8*, *Insr*, and *Cotl1*, which showed hypermethylation of their gene bodies, displayed upregulation of gene expression in MS.

Analysis of DMRs

Next, we determined the DMR, which constitutes consecutive CpG sites covering significant genomic regions. A total of 151 DMRs were identified in MS, including 65 hypomethylated and 86 hypermethylated regions with a methylation difference of |

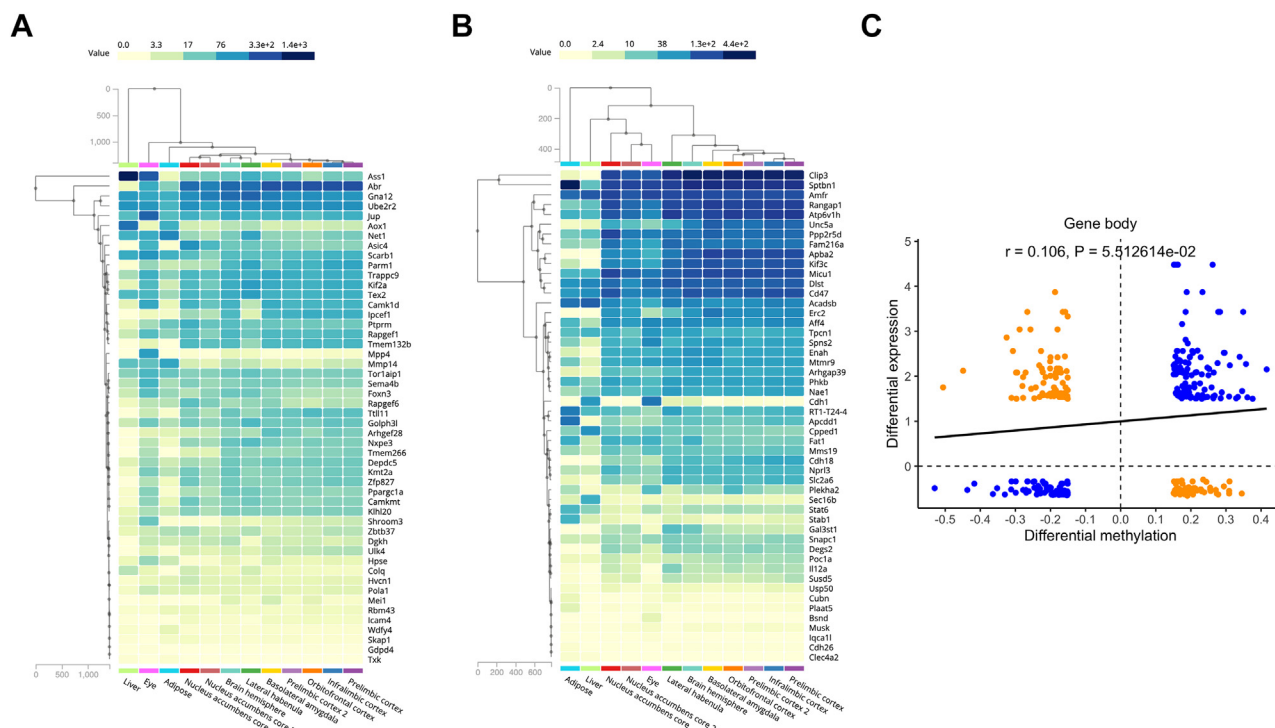


Figure 6. The gene expression profile of the top 50 DMCs containing genes obtained from the RatGTEx database. **(A)** Strong hypomethylated. **(B)** Strong hypermethylated. **(C)** Correlation of methylation levels with expression profile of genes with gene body DMCs. Scatter plot and Pearson's correlation showing the correlation between the differences in mRNA expression and methylation. The line represents a linear regression. Blue and orange dots represent the mRNA-DMC pairs exhibiting positive or inverse relationships, respectively. DMC, differentially methylated cytosine; mRNA, messenger RNA.

0.2] (Figure 7A and Table S12). The regions spanned a total 10 kb of genome, ranging from 8 to 519 bp in length. The methylation level of the top 50 DMRs across the control and MS samples is provided as a heatmap (Figure 7B). DMRs were observed across all chromosomes with the exception of chromosome Y (Figure 7C, D and Supplement). Most of the DMRs were situated within genic coordinates (enriched, $p = 2.7 \times 10^{-5}$), while the fewest were found in the promoter region (Figure 7E; Tables S13 and S14; Supplement). Also, the CpG island harbored 36 DMRs and the shore region had 27, and 8.6% of the identified DMRs were located in the CpG shelf (Figure 7F).

Functional Analysis of Genes Present in DMRs

Functional analysis of genes present in both hyper- and hypo-DMRs was performed. It was found that the genes in hypo-DMRs had enrichment of the MAPK signaling pathway (Figure 8A). In terms of biological processes, the genes were linked to ribonucleoprotein complex biogenesis, sodium ion transmembrane transport, and response to gonadotropin (Figure 8B). Among molecular function, an enrichment for sodium ion transmembrane activity, MAPK kinase activity, and voltage-gated sodium ion channel activity was observed (Figure 8C and Table S15).

The genes within the hyper-DMRs were associated with the AMPK, oxytocin signaling, and glutamatergic synapse pathways (Figure 8D). Among the biological process terms, genes associated with neural precursor cell proliferation and central

nervous system neuron differentiation were enriched (Figure 8E). The molecular functions of the genes present in hypermethylated regions were linked to DNA binding transcription activator activity, β -catenin binding, and transcription coregulator binding activity (Figure 8F and Table S16).

Tissue-Level Expression Analysis of DMR Genes

The expression analysis of genes in DMRs from the RatGTEx portal in normal tissues showed that the genes *Gna12*, *Ssbp3*, *Negr1*, *Eri3*, and *Slc2a3* within hypo-DMRs had higher expression in various brain tissues. The hypo-DMRs in the gene body may decrease the expression of these genes. Additionally, genes from hyper-DMRs, such as *Rora* and *Sox5*, exhibited consistently lower expression across all brain tissues, and the hypermethylated sites may increase the expression of these genes in MS (Figure 9A, B and Table S17).

The *Rps19* gene, the only promoter in the hypo-DMR, showed higher expression in all brain tissues. The expression of *Cpeb2* and *Ptpn18* genes, which were regulated by the hyper-DMR in the promoter, demonstrated lower expression across all tissues except for *Pcbp4*, which exhibited higher expression in all brain tissues (Figure 9C and Table S18).

Enrichment of TFBSs

The epigenetic regulation of crucial TFBSs can govern the expression of downstream signaling genes, leading to profound alterations in behavioral changes during MS. The

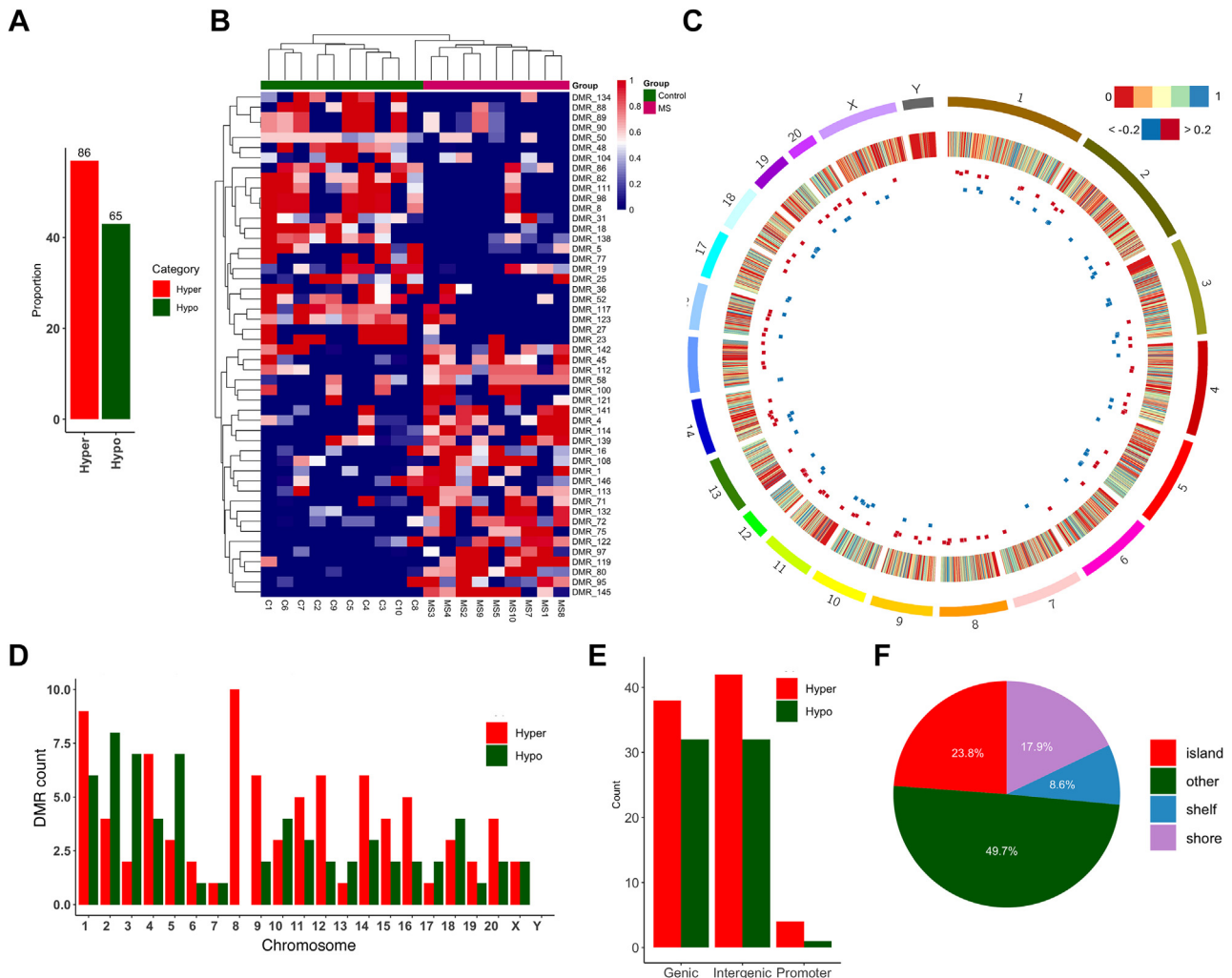


Figure 7. DMRs. **(A)** The distribution of the hyper- and hypomethylated sites among all 151 significant DMRs. **(B)** Heatmap depicting the methylation levels of the top 50 DMRs between MS and control groups. The samples and differentially methylated cytosine sites were clustered using the hierarchical clustering algorithm. **(C)** Circos plot depicting the DMR across the chromosome. Gene density within 500-kb window is plotted in the first track and the DMR distribution. The hypermethylated regions are colored red, and the hypomethylated DMRs are plotted as blue. **(D)** The distribution of hyper- and hypomethylated regions in rat chromosomes. **(E)** The distribution of DMRs in the genic, intergenic, and promoter regions. **(F)** The distribution of DMRs in the CpG island, shore, shelf, and other regions. C, control; DMR, differentially methylated region; MS, maternal separation.

enriched motifs identified in DMRs included C2H2 zinc finger factors: *Zic1*:*Zic2*, *Lhx6*, and *Lhx3* transcription factors and ETS (E26 transformation-specific) transcription factors *Elk1* and *Elk4* (Figure S3A and Table S19).

Gene Interaction Network Analysis

The gene interaction network offers insight into the regulatory cascade and biological implications of differential methylation. Among the genes regulated by the differentially methylated promoters, the strong hypomethylated promoters had known interaction between *Rps19*, *Rpl10*, and *Mrps5*—genes associated with protein translation (Figure S3B). Conversely, the genes regulated by hypermethylated promoters revealed an interplay between MAPK signaling pathway genes, *Mapk14* and *Mef2c*, and actin cytoskeleton genes, including *Actc1*,

Actb, and *Myh6* (Figure S3C). In the context of genes present in hypo-DMRs, an interaction between *Zfp407* and *Gna12* was identified (Figure S3D). Conversely, the genes from hyper-DMRs exhibited one-on-one interactions involving *Rab6b* and *Ephb1*, *Sox5* and *Foxp1*, *Foxo3* and *Axin2*, *Brsk2* and *Camkk2*, and *Fnib* and *Nfix* genes (Figure S3E). The genes that harbored strong hypo- and hyper-DMCs in the gene loci displayed a subnetwork of 17 and 12 genes, respectively (Figure S4 and Supplement).

Differentially Methylated Non-CpG Sites

Apart from CpG dinucleotides, methylation also occurs in non-CpG sites, including CHG and CHH, where H represents A, T, or C. Therefore, in the current study, we examined DNA methylation on both these non-CpG sites.

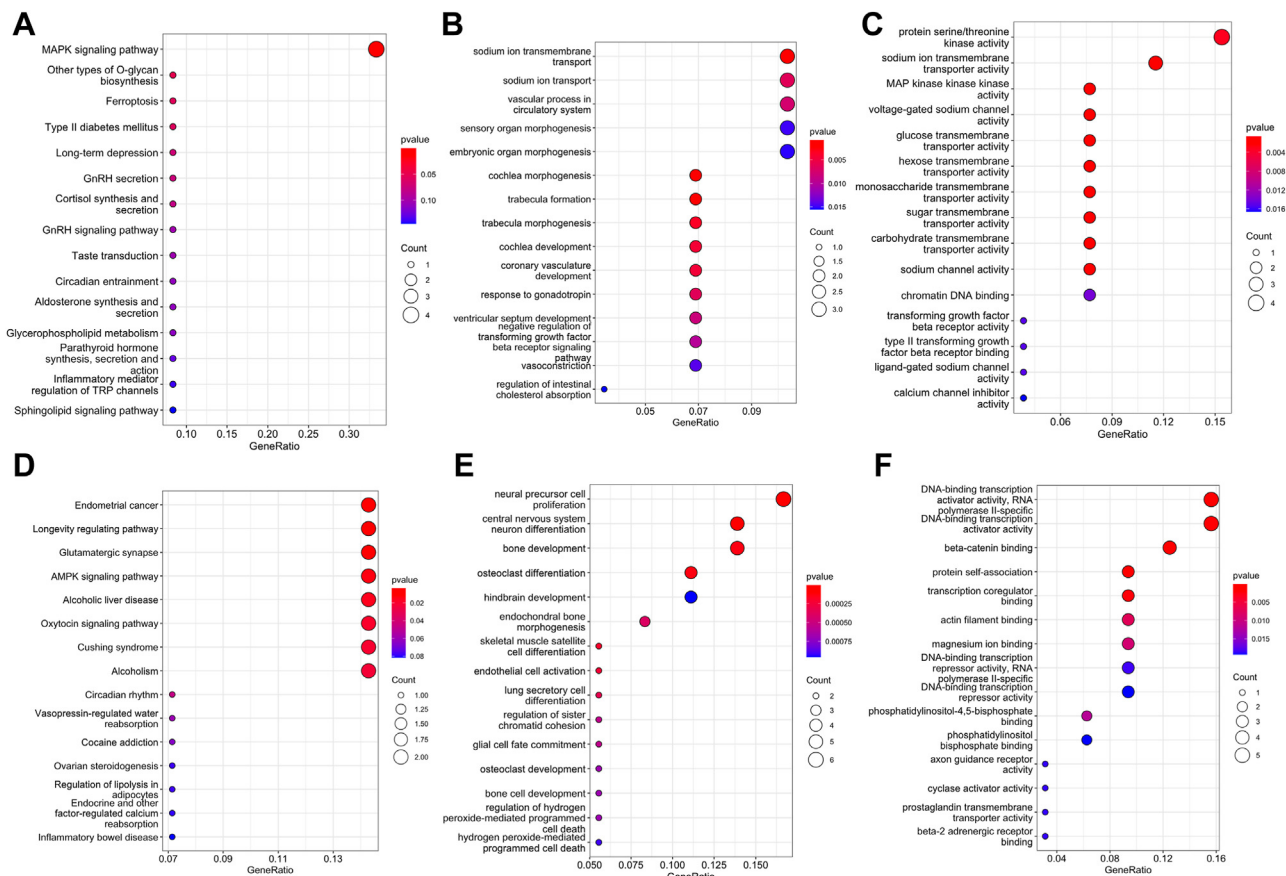


Figure 8. Functional enrichment analysis of the genes present in the significant differentially methylated regions. **(A)** The KEGG pathways enriched among the genes present in strong hypomethylated regions. **(B)** The biological process enriched among the genes present in strong hypomethylated regions. **(C)** The enriched molecular function terms among the genes present in strong hypomethylated regions. **(D)** The KEGG pathways enriched among the genes present in strong hypermethylated regions. **(E)** The biological process enriched among the genes present in strong hypermethylated regions. **(F)** The enriched molecular function terms among the genes present in strong hypermethylated regions. GnRH, gonadotropin-releasing hormone; KEGG, Kyoto Encyclopedia of Genes and Genomes; MAPK, mitogen-activated protein kinase; TRP, transient receptor potential.

Differentially Methylated CHG Sites. Approximately 48 million CHG sites were identified in the PFC of both control and MS rats. However, only 938 CHG sites were found to be differentially regulated with MS (Figure 10A and Table S20). The distribution of differential CHG sites across the chromosome shows that chromosome 19 contained 70 strongly hypomethylated sites, while most of the other chromosomes displayed a hypermethylation pattern (Figure 10B). Among the differentially methylated CHG sites, 14 covered 13 gene promoters, and 285 sites were located within 272 gene loci (Tables S21 and S22). The functional enrichment analysis yielded no significant results for both promoters and genes.

Differentially Methylated CHH Sites. Differential methylation analysis between the control and MS groups identified 4926 significant CHH sites across the genome (Table S23). Most were hypomethylated, followed by hypermethylated sites (Figure 10C). Across all chromosomes, hypomethylated CHH sites were predominant, and

chromosome 1 harbored a maximum number of differentially methylated sites (84 sites); the least number of sites were present in chromosome Y (Figure 10D).

Genes Linked to Differentially Methylated CHH Sites. Of the differential CHH sites identified, 102 were situated within the promoters of 99 genes, while 1810 were located in the gene loci of 1338 genes. Among the genes with differential methylation at the CHH site in the gene body, 576 sites were hypomethylated, and 304 were hypermethylated. Also, only 143 genes showed strong hypermethylation, and 315 genes showed strong hypomethylation (Table S24).

The functional enrichment analysis of genes with strong differentially methylated CHH sites within the gene body revealed that hypo-CHH-containing genes were enriched for Wnt signaling pathways (Figure 11A). Conversely, genes with hyper-CHH sites in gene loci were associated with axon guidance and calcium signaling pathways (Figure 11B). The enriched biological processes indicated that the genes with hypo-CHH sites were involved in cell junction assembly, axon

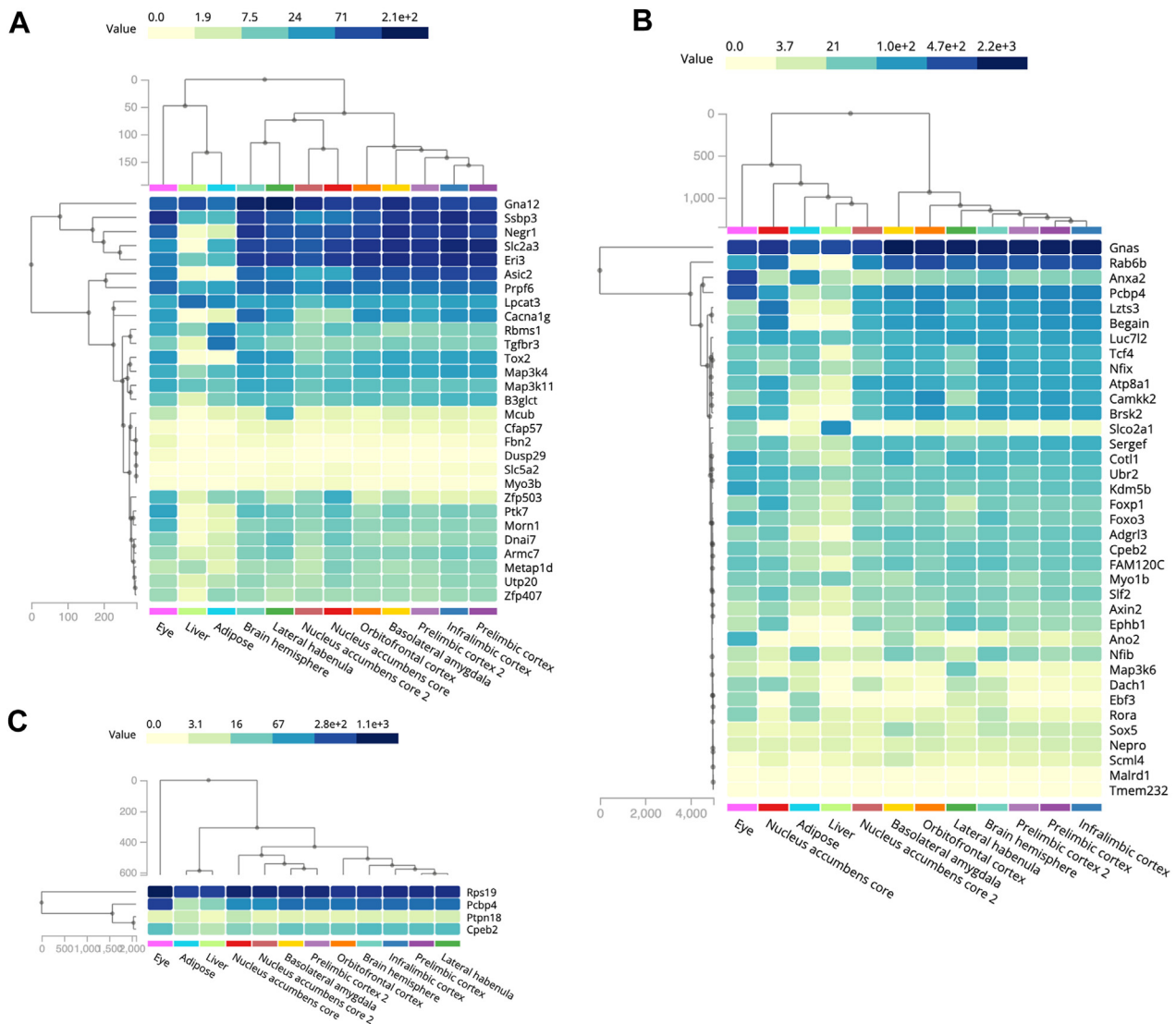


Figure 9. (A) The gene expression profile of the genes present in the top 50 DMRs, obtained from the RatGTEx database. (A) Strong hypomethylated. (B) Strong hypermethylated. (C) The gene expression profile of the DMR hypermethylated promoters regulating *Pcbp4*, *Ptpn18*, and *Cpeb2* and also the hypomethylated promoter of the *Rps19* gene. DMR, differentially methylated region.

guidance, neuron projection guidance, and myelination (Figure 11C). In contrast, the genes that had hyper-CHH sites showed involvement in small GTPase-mediated signal transduction, positive regulation of cell projection organization, synapse maturation, and long-term synaptic potentiation (Figure 11D). Also, the molecular function terms enriched show the actin-binding, cadherin binding, and sodium channel regulator activity terms among genes with hypo-CHH sites (Figure 11E), while cyclase activity, MAPK kinase binding activity, and calcium-activated cation channel activity were identified among hyper-CHH sites containing genes (Figure 11F; Tables S25 and S26). The complete list of promoters with differential CHH sites is provided in Table S27, but the functional enrichment analysis yielded no significant results.

DISCUSSION

The findings from the current study highlight the profound impact of early-life stress (ELS), particularly when viewed from the perspective of the MS model, on the epigenetic landscape of the brain. The observation of reduced sucrose preference in rats subjected to MS serves as a compelling indicator of anhedonia. This behavioral change underscores the necessity of further investigating the epigenetic modifications that accompany such early-life stressors. The delineation of methylation patterns in the control and MS groups provides critical insight into the epigenetic imprinting related to ELA. The prevalence of widespread DNA methylation changes at both CpG and non-CpG sites suggests a comprehensive reprogramming of the genomic landscape influenced by stress. The

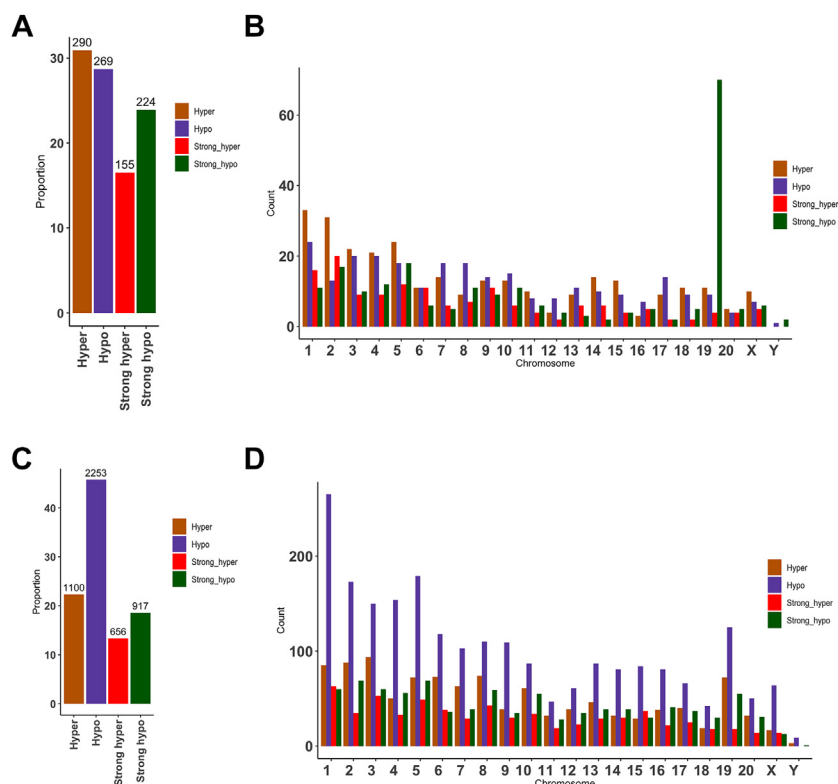


Figure 10. Non-CpG site methylation analysis. **(A)** The distribution of hyper- and hypomethylated sites among all 938 significant CHG DMCs. **(B)** The distribution of hyper- and hypomethylated CHG sites across rat chromosomes. **(C)** The distribution of hyper- and hypomethylated sites among all 4926 significant CHH DMCs. **(D)** The distribution of hyper- and hypomethylated CHH sites across rat chromosomes. DMC, differentially methylated cytosine.

predominance of hypermethylation over hypomethylation, especially at CpG sites, raises important questions about how these modifications may inhibit necessary gene expression linked to neurodevelopment and stress response. Moreover, the enrichment of differentially methylated genes in pathways essential for synaptic function and neurodevelopment reflects how ELS may disrupt critical processes in brain development and function. The identification of DMRs, particularly those located within gene bodies, may indicate functional implications for gene expression regulation. Furthermore, the analysis revealed alterations in TFBSs and gene interaction networks, suggesting that ELS does not merely cause isolated gene-specific changes but rather leads to broader disruptions in cellular processes that govern brain function. Such disruptions may have far-reaching implications, potentially paving the way for the development of stress-related disorders.

The genes subjected to regulation by differential methylation offer valuable insights into the dysregulation of biological pathways and functions through epigenetic mechanisms. Hypomethylated CpG sites located in the promoter region may enhance the expression of the corresponding genes. The *Notch1* gene, with a hypomethylated promoter in MS, has shown upregulation of the transcript in the hippocampus during the long MS, implicating the relevance of the *Notch1* system in neural development or disorders (30). Strong hypomethylation of the promoter region was observed for the *Grin3b* gene. Previous research indicates that blood messenger RNA levels of *GRIN3B* hold promise as an early

biomarker for diagnosing and understanding the development of posttraumatic stress disorder (31).

Considering that hypermethylation of promoters is linked to reduced gene expression, it is essential to investigate the functions of these potentially downregulated genes. The strong hyper-DMCs in promoters that regulate motor proteins such as *Kif4a*, *Actc1*, and *Actb* could lead to axonal transport deficits and contribute to the dysregulation of synapse plasticity, neuronal function, learning, and memory, as has been observed in several neuropsychiatric disorders (32). The anxiety disorder genes *CCKBR* and *MEF2C*, involved in positive regulation of the behavioral fear response, showed a strong hypermethylation pattern, and they have been found to overlap with schizophrenia and bipolar disorder, respectively (33).

The substantial number of genes that displayed gene body methylation warrants further investigation into the functional implications, particularly considering the contrasting effect of gene body methylation on gene expression compared with promoters. Our study revealed notable epigenetic modifications encompassing both hypo- and hyper-DMCs within the gene bodies of MAPK and cholinergic synapse pathway genes. As detailed in [Supplemental Discussion](#), both pathways are linked to the pathophysiology of depression, highlighting the intricate nature of epigenetic regulation through gene body methylation in MS.

Consecutively methylated CpG sites within DMRs are more likely to be associated with altered gene expression and have a substantial impact on disease phenotype than methylation at a single site (34). The hyper-DMRs in the promoter region of RNA

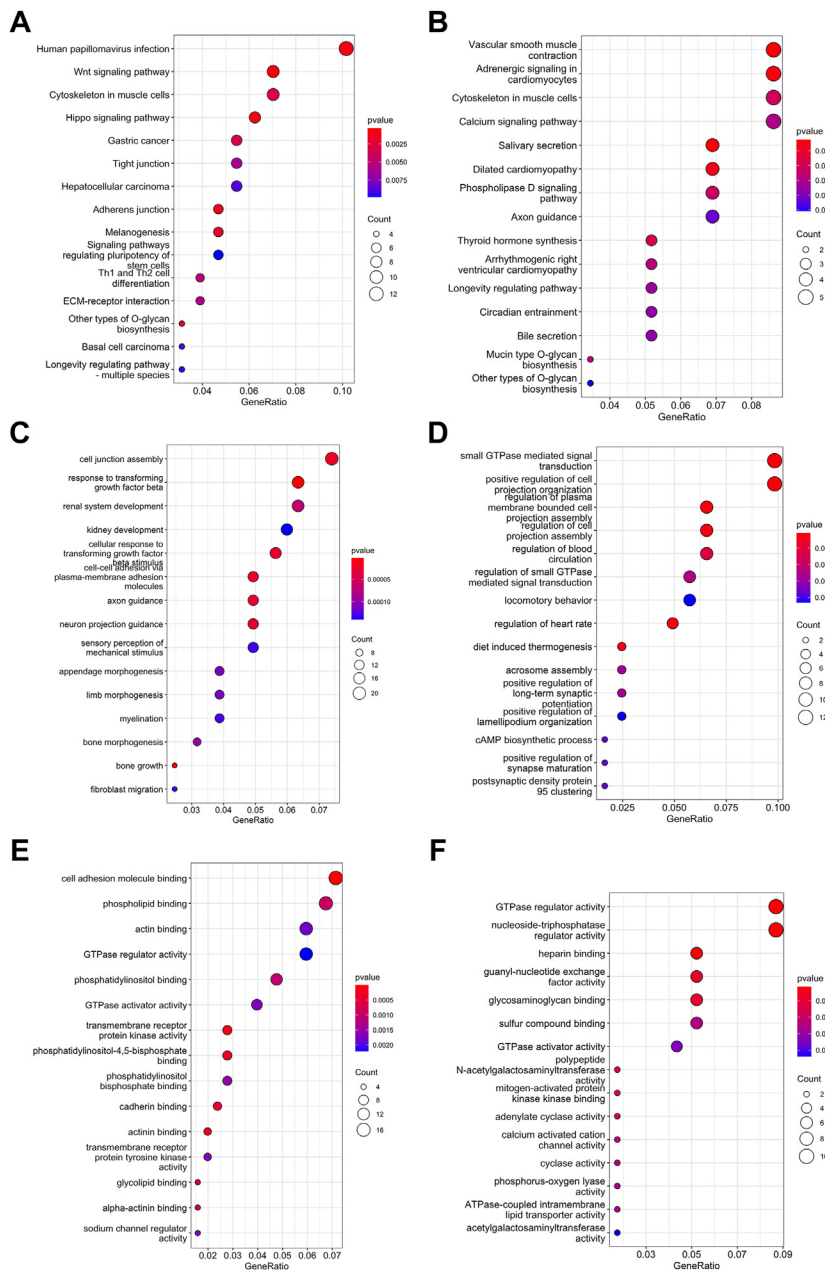


Figure 11. The functional analysis of the genes with differentially methylated cytosines at the CHH site. **(A)** The KEGG pathways enriched among the genes having strong hypomethylation. **(B)** The KEGG pathways enriched among the genes having strong hypermethylation. **(C)** The enriched biological process terms among the genes having strong hypomethylated cytosines. **(D)** The enriched biological process terms among the genes having strong hypermethylation cytosines. **(E)** The enriched molecular function terms among the genes having strong hypomethylated cytosines. **(F)** The enriched molecular function terms among the genes having hypermethylation cytosines. ATPase, adenosine triphosphatase; cAMP, cyclic adenosine monophosphate; ECM, extracellular matrix; GTPase, guanosine triphosphatase; KEGG, Kyoto Encyclopedia of Genes and Genomes.

binding protein *Pcbp4* and the hypo-DMRs in ribosomal gene *Rps19* are noteworthy. The connection between these genes and neurotransmitter signaling and ribosomal dysfunction is further elaborated in [Supplemental Discussion](#). DMR hypomethylation within the gene body was observed for *Gna12*, and the dysregulated *GNA12* G α subunit is shared by autism spectrum disorder, schizophrenia, and bipolar disorder (35). Our study identified another G protein, *Gnas*, which is

associated with a hyper-DMR, and this finding is consistent with a previous anxiety-related hyper-DMR that has been identified (36). Moreover, the consistently higher expression of both *Gna12* and *Gnas* across multiple brain tissues underscores the potential functional relevance of these genes in the brain.

The observed methylation changes in TFBSs highlight a significant mechanism through which gene expression can be

regulated in the context of brain development and behavioral alterations associated with MS. The enrichment of specific TFBSs, such as the zinc finger factors *Zic1*, *Zic2*, and *Lhx6*, together with *Lhx3* and the ETS factors *Elk1* and *Elk4*, signals a critical adaptation in the gene regulatory networks of MS rats. *Zic2* and *Lhx6* are involved in forebrain neuron development, whereas *Lhx3* is required for motor neuron specification. Interestingly, ELK-1 TF is upregulated in deaths by suicide related to depression and animal models of depression induced by unpredictable chronic mild stress and social defeat (37). Notably, patients who responded positively to antidepressant treatment had significantly lower blood levels of ELK-1 than nonresponders (37).

The gene interaction network offers insight into the regulatory cascade and biological implications of differential methylation. The hypermethylated DMRs identified within the gene loci of TF *Foxp1* and the interacting partner *Sox5* are significant because *FOXP1* is closely associated with human neurodevelopmental disorders, including intellectual disability, autism spectrum disorder, and speech and language disorders (38). The genes that harbored strong hypo-DMCs in the gene loci displayed a subnetwork of genes that are integral to the voltage-gated calcium channel complex that governs presynaptic depolarization and calcium channel opening. This complex plays a critical role in neurotransmitter release and has also been linked to various neuropsychiatric disorders, including depression, autism, schizophrenia, cerebellar ataxia, and bipolar disorder (39–41). Interestingly, interactions among various genes that had hyper-DMCs in the gene body formed a network, including glutamate-related genes that act as Glu receptors in tripartite glutamate synapse. The association of AMPA receptors (*GRIA3* and *GRIA4*), kainate receptors (*GRIK2* and *GRIK2*), and NMDA receptors (*GRIN2A* and *GRIN2B*) in the pathophysiology of mood disorders has been established (42).

It has been reported that non-CpG methylation is associated with transcriptional repression and the pluripotency-associated epigenetic state (43,44). This supports the notion that non-CpG methylation is an emerging epigenetic marker for defining tissue-specific patterns of gene expression, particularly in the brain. Because the majority of the identified non-CpG sites were of the CHH type, CHH site methylation likely has a more pronounced impact on gene expression regulation than CHG in MS. The role of non-CpG methylation in gene regulation and its link to psychiatric disorders is discussed further in [Supplemental Discussion](#).

Conclusions

The current study provides a comprehensive analysis of DNA methylation changes in the rat brain following MS, an established model of ELS. These epigenetic alterations have the potential to significantly impact gene expression and contribute to the development of stress-related psychiatric disorders in adulthood. We observed widespread alterations in genes that are critical for neurodevelopment, synaptic function, and the stress response that occur through methylation at both CpG and non-CpG sites in the promoter regions and gene bodies. The pathways and gene interactions that we identified are highly relevant to the

underlying mechanisms of stress-related disorders, such as depression and anxiety. One limitation is that we only found subtle behavioral effects except for changes in sucrose preference/anhedonia. MS has been shown to lead to a variety of behavioral changes, with some inconsistencies in the literature (45–48). Because we only found anhedonia-like behavior, our epigenetic data are likely most relevant to this facet of ELS. The lack of other behavioral findings might have resulted from lower sample sizes and reduced power to detect differences in the forced swim and elevated plus maze tests. Future well-powered studies should test the direct association between epigenetic changes and anxiety-like behaviors related to ELS. Moreover, it is essential to recognize that this investigation was confined to the PFC, implying that patterns of epigenetic dysregulation may vary across different brain regions. Lastly, future studies should focus on validating these methylation changes and exploring their functional consequences on gene expression and behavior. Additionally, investigating the reversibility of these epigenetic modifications may open new avenues for interventions for stress-related psychopathologies.

ACKNOWLEDGMENTS AND DISCLOSURES

YD is supported by the National Institute of Mental Health (Grants Nos. R01MH130539, R01MH124248, R01MH118884, R01MH128994, R01MH107183, and R56MH138596).

YD conceptualized the study, LAM performed the experiments, and AF analyzed the data. All authors cowrote the draft of the article, which YD edited and finalized.

All data are provided in the article.

The authors report no biomedical financial interests or potential conflicts of interest.

ARTICLE INFORMATION

From the Department of Psychiatry and Behavioral Neurobiology, Heersink School of Medicine, University of Alabama at Birmingham, Birmingham, Alabama (AF, YD); and Institute for Trauma Recovery, Department of Anesthesiology, University of North Carolina School of Medicine, University of North Carolina at Chapel Hill, Chapel Hill, North Carolina (LAM).

Address correspondence to Yogesh Dwivedi, Ph.D., at ydwivedi@uab.edu.

Received Dec 13, 2024; revised Feb 21, 2025; accepted Mar 1, 2025.

Supplementary material cited in this article is available online at <https://doi.org/10.1016/j.bpsgos.2025.100487>.

REFERENCES

- Ochi S, Dwivedi Y (2023): Dissecting early life stress-induced adolescent depression through epigenomic approach. *Mol Psychiatry* 28:141–153.
- Howell BR, Grand AP, McCormack KM, Shi YD, LaPrairie JL, Maestripieri D, et al. (2014): Early adverse experience increases emotional reactivity in juvenile rhesus macaques: Relation to amygdala volume. *Dev Psychobiol* 56:1735–1746.
- Kessler RC, McLaughlin KA, Green JG, Gruber MJ, Sampson NA, Zaslavsky AM, et al. (2010): Childhood adversities and adult psychopathology in the WHO World Mental Health Surveys. *Br J Psychiatry* 197:378–385.
- Hillis S, Mercy J, Amobi A, Kress H (2016): Global prevalence of past-year violence against children: A systematic review and minimum estimates. *Pediatrics* 137:e20154079.
- Giano Z, Wheeler DL, Hubach RD (2020): The frequencies and disparities of adverse childhood experiences in the U.S. *BMC Public Health* 20:1327.

6. Dutcher EG, Pama EAC, Lynall ME, Khan S, Clatworthy MR, Robbins TW, *et al.* (2020): Early-life stress and inflammation: A systematic review of a key experimental approach in rodents. *Brain Neurosci Adv* 4:2398212820978049.
7. Smith KE, Pollak SD (2020): Early life stress and development: Potential mechanisms for adverse outcomes. *J Neurodev Disord* 12:34.
8. Nakama N, Usui N, Doi M, Shimada S (2023): Early life stress impairs brain and mental development during childhood increasing the risk of developing psychiatric disorders. *Prog Neuropsychopharmacol Biol Psychiatry* 126:110783.
9. McLaughlin K (2020): Early life stress and psychopathology. In: Harkness KL, Hayden EP, editors. *The Oxford Handbook of Stress and Mental Health*. Oxford, England: Oxford University Press, 45–74.
10. Pechtel P, Pizzagalli DA (2011): Effects of early life stress on cognitive and affective function: An integrated review of human literature. *Psychopharmacology* 214:55–70.
11. Kessler RC, Davis CG, Kendler KS (1997): Childhood adversity and adult psychiatric disorder in the US National comorbidity Survey. *Psychol Med* 27:1101–1119.
12. Haller J, Harold G, Sandi C, Neumann ID (2014): Effects of adverse early-life events on aggression and anti-social behaviours in animals and humans. *J Neuroendocrinol* 26:724–738.
13. Na KS, Jung HY, Kim YK (2014): The role of pro-inflammatory cytokines in the neuroinflammation and neurogenesis of schizophrenia. *Prog Neuropsychopharmacol Biol Psychiatry* 48:277–286.
14. Chen GP, Zhang YH, Li RL, Jin LY, Hao KK, Rong JT, *et al.* (2024): Environmental enrichment attenuates depressive-like behavior in maternal rats by inhibiting neuroinflammation and apoptosis and promoting neuroplasticity. *Neurobiol Stress* 30:100624.
15. Zhang Y, Wang S, Hei MY (2024): Maternal separation as early-life stress: Mechanisms of neuropsychiatric disorders and inspiration for neonatal care. *Brain Res Bull* 217:111058.
16. Rahman MF, McGowan PO (2022): Cell-type-specific epigenetic effects of early life stress on the brain. *Transl Psychiatry* 12:326.
17. Wang FS, Pan F, Tang YY, Huang JH (2021): Editorial: Early life stress-induced epigenetic changes involved in mental disorders. *Front Genet* 12:684844.
18. Alyamani RAS, Murgatroyd C (2018): Epigenetic programming by early-life stress. *Prog Mol Biol Transl Sci* 157:133–150.
19. Allen L, Dwivedi Y (2020): MicroRNA mediators of early life stress vulnerability to depression and suicidal behavior. *Mol Psychiatry* 25:308–320.
20. Wang Q, Xiong F, Wu GH, Liu WZ, Chen JS, Wang B, Chen Y (2022): Gene body methylation in cancer: Molecular mechanisms and clinical applications. *Clin Epigenetics* 14:154.
21. McCoy CR, Rana S, Stringfellow SA, Day JJ, Wyss JM, Clinton SM, Kerman IA (2016): Neonatal maternal separation stress elicits lasting DNA methylation changes in the hippocampus of stress-reactive Wistar Kyoto rats. *Eur J Neurosci* 44:2829–2845.
22. Park SW, Seo MK, Lee JG, Hien LT, Kim YH (2018): Effects of maternal separation and antidepressant drug on epigenetic regulation of the brain-derived neurotrophic factor exon I promoter in the adult rat hippocampus. *Psychiatry Clin Neurosci* 72:255–265.
23. McKibben LA, Dwivedi Y (2021): MicroRNA regulates early-life stress-induced depressive behavior via serotonin signaling in a sex-dependent manner in the prefrontal cortex of rats. *Biol Psychiatry Glob Open Sci* 1:180–189.
24. Timberlake M, Roy B, Dwivedi Y (2019): A novel animal model for studying depression featuring the induction of the unfolded protein response in hippocampus. *Mol Neurobiol* 56:8524–8536.
25. Primo MJ, Fonseca-Rodrigues D, Almeida A, Teixeira PM, Pinto-Ribeiro F (2023): Sucrose preference test: A systematic review of protocols for the assessment of anhedonia in rodents. *Eur Neuropsychopharmacol* 77:80–92.
26. Kraeuter AK, Guest PC, Samyaz Z (2019): The elevated plus maze test for measuring anxiety-like behavior in rodents. *Methods Mol Biol* 1916:69–74.
27. Yankelevitch-Yahav R, Franko M, Huly A, Doron R (2015): The forced swim test as a model of depressive-like behavior. *J Vis Exp* 97:e52587.
28. Benekareddy M, Goodfellow NM, Lambe EK, Vaidya VA (2010): Enhanced function of prefrontal serotonin 5-HT(2) receptors in a rat model of psychiatric vulnerability. *J Neurosci* 30:12138–12150.
29. Heinz S, Benner C, Spann N, Bertolino E, Lin YC, Laslo P, *et al.* (2010): Simple combinations of lineage-determining transcription factors prime cis-regulatory elements required for macrophage and B cell identities. *Mol Cell* 38:576–589.
30. Steine IM, Zayats T, Stansberg C, Pallesen S, Mrdalj J, Håvik B, *et al.* (2016): Implication of NOTCH1 gene in susceptibility to anxiety and depression among sexual abuse victims. *Transl Psychiatry* 6:e977.
31. Lori A, Schultebrasucks K, Galatzer-Levy I, Daskalakis NP, Katrinli S, Smith AK, *et al.* (2021): Transcriptome-wide association study of post-trauma symptom trajectories identified GRIN3B as a potential biomarker for PTSD development. *Neuropsychopharmacology* 46:1811–1820.
32. Badal KK, Puthanveetil SV (2022): Axonal transport deficits in neuropsychiatric disorders. *Mol Cell Neurosci* 123:103786.
33. Le-Niculescu H, Balaraman Y, Patel SD, Ayalew M, Gupta J, Kuczenski R, *et al.* (2011): Convergent functional genomics of anxiety disorders: Translational identification of genes, biomarkers, pathways and mechanisms. *Transl Psychiatry* 1:e9.
34. Jaffe AE, Murakami P, Lee H, Leek JT, Fallin MD, Feinberg AP, Irizarry RA (2012): Bump hunting to identify differentially methylated regions in epigenetic epidemiology studies. *Int J Epidemiol* 41:200–209.
35. Monfared RV, Alhassen W, Truong TM, Gonzales MAM, Vachirakornpong V, Chen SW, *et al.* (2021): Transcriptome profiling of dysregulated GPCRs reveals overlapping patterns across psychiatric disorders and age-disease interactions. *Cells* 10:2967.
36. Alisch RS, Van Hulle C, Chopra P, Bhattacharyya A, Zhang SC, Davidson RJ, *et al.* (2017): A multi-dimensional characterization of anxiety in monozygotic twin pairs reveals susceptibility loci in humans. *Transl Psychiatry* 7:1282.
37. Apazoglou K, Farley S, Gorgievski V, Belzeaux R, Lopez JP, Grenier J, *et al.* (2018): Antidepressive effects of targeting ELK-1 signal transduction. *Nat Med* 24:591–597.
38. Co M, Anderson AG, Konopka G (2020): FOXP transcription factors in vertebrate brain development, function, and disorders. *Wiley Interdiscip Rev Dev Biol* 9:e375.
39. Nanou E, Catterall WA (2018): Calcium channels, synaptic plasticity, and neuropsychiatric disease. *Neuron* 98:466–481.
40. Zamponi GW (2016): Targeting voltage-gated calcium channels in neurological and psychiatric diseases. *Nat Rev Drug Discov* 15:19–34.
41. Andrade A, Brennecke A, Mallat S, Brown J, Gomez-Rivadeneira J, Czepl N, Londrigan L (2019): Genetic associations between voltage-gated calcium channels and psychiatric disorders. *Int J Mol Sci* 20:3537.
42. Sequeira A, Mamdani F, Ernst C, Vawter MP, Bunney WE, Lebel V, *et al.* (2009): Global brain gene expression analysis links glutamatergic and GABAergic alterations to suicide and major depression. *PLoS One* 4:e6585.
43. Guo JU, Su YJ, Shin JH, Shin JH, Li HD, Xie B, *et al.* (2014): Distribution, recognition and regulation of non-CpG methylation in the adult mammalian brain. *Nat Neurosci* 17:215–222.
44. Ma H, Morey R, O'Neil RC, He YP, Daughtry B, Schultz MD, *et al.* (2014): Abnormalities in human pluripotent cells due to reprogramming mechanisms. *Nature* 511:177–183.
45. Duque-Wilckens N, Teis R, Sarno E, Stoelting F, Khalid S, Dairi Z, *et al.* (2022): Early life adversity drives sex-specific anhedonia and meningeal immune gene expression through mast cell activation. *Brain Behav Immun* 103:73–84.
46. Francis-Oliveira J, Shieh IC, Vilar Higa GS, Barbosa MA, De Pasquale R (2021): Maternal separation induces changes in TREK-1 and 5HT1A expression in brain areas involved in the stress response in a sex-dependent way. *Behav Brain Res* 396:112909.
47. Genty J, Tetsi Nomigni M, Anton F, Hanesch U (2018): The combination of postnatal maternal separation and social stress in young adulthood does not lead to enhanced inflammatory pain sensitivity and depression-related behavior in rats. *PLoS One* 13:e0202599.
48. Andersen SL (2015): Exposure to early adversity: Points of cross-species translation that can lead to improved understanding of depression. *Dev Psychopathol* 27:477–491.